Journal of Molecular Catalysis A: Chemical 378 (2013) 344–349

Contents lists available at SciVerse ScienceDirect

Journal of Molecular Catalysis A: Chemical

journal homepage: www.elsevier.com/locate/molcata

A hierarchical Fe_3O_4@P4VP@$MoO_2(acac)_2$ nanocomposite: Controlled synthesis and green catalytic application

Wanchun Guo [a], Ge Wang [a,*], Qian Wang [a], Wenjun Dong [a], Mu Yang [a], Xiubing Huang [a], Jie Yu [a], Zhan Shi [b]

[a] School of Materials Science and Engineering, University of Science and Technology Beijing, Beijing 100083, PR China
[b] State Key Laboratory of Inorganic Synthesis and Preparative Chemistry, College of Chemistry, Jilin University, Changchun 130012, PR China

ARTICLE INFO

Article history:
Received 31 October 2012
Received in revised form 22 March 2013
Accepted 18 April 2013
Available online 25 April 2013

Keywords:
Magnetite/poly(4-vinylpyridine) nanospheres
Epoxidation
Catalysis
Magnetic recovery
Superparamagnetism

ABSTRACT

Magnetite/poly(4-vinylpyridine) composite nanospheres with multiple Fe_3O_4 cores embedded in a P4VP shell were first synthesized by miniemulsion polymerization and then used as recoverable supports for $MoO_2(acac)_2$ complex. The supported complex, together with superparamagnetism and strong magnetic response, showed high efficiency for the catalytic epoxidation of cis-cyclooctene with aqueous H_2O_2 in ethanol. The response strongly facilitated the easy recovery of the catalyst, which was stable in recycling tests.

1. Introduction

High dispersion and easy recoverability of heterogeneous catalyst in liquid-phase reaction are of great importance in order to achieve high efficiency and effective reuse. Classical micrometre-size heterogeneous catalysts are recoverable [1], but have significantly reduced reaction activity or selectivity due to low dispersion in the liquid-phase systems, the low concentration of active sites, and difficult access for reactants and products to active sites deep inside the support [2]. With the development of nanotechnology during the last decade, various nanoscale polymeric and inorganic supports with a large surface area have been synthesized to raise homogeneous catalyst loading and catalytic activity [3,4]. Especially, complex catalysts grafted on nanoparticles in liquid-phase system exhibit excellent activity similar to the equivalents since the active sites located on the surface of the nanoparticles are easily accessible to reactants at a molecular level. Unfortunately, conventional separation techniques such as filtration and centrifugation may become insufficient for support particles less than 100 nm in diameter. Magnetic nanoparticles incorporated into supports provide a practical route to overcome this drawback. Various composite supports with magnetic nanoparticles encapsulated in inorganic or polymeric matrixes have been developed to immobilize catalyst for application in liquid reaction [5–7].

However, there are still some problems such as the low magnetic content and high remanence of most magnetic composite supports, as reported previously. A low magnetic content of composite supports results in a weak response affecting the recovery efficiency of nanocatalysts, while a high remanence of those leads to their possible coagulation during the catalytic transformation. As a result, how to obtain nanocomposite supports with a strong magnetic response and superparamagnetism as well is still a challenge. Superparamagnetic inorganic/polymer composite nanospheres, which are usually composed of abundant magnetic cores to ensure a strong magnetic response and polymeric shells to provide favourable functional groups and get rid of magnetic particle aggregation, may provide an opportunity to solve this problem. Maintaining their high activity, homogeneous catalysts anchored on composite nanospheres may be recovered easily and rapidly upon a moderate magnetic field. Superparamagnetic composite nanospheres (e.g., Fe_3O_4/polystyrene) with narrow size distribution, magnetic cores homogenously distributed into polymer matrixes and a high magnetite fraction (from 70%, up to 80%, respectively), have been prepared successfully by miniemulsion polymerization [8,9], but further surface modification of composite nanospheres under harsh conditions may destroy their magnetism before firm immobilization of transition-metal complex catalysts [10]. This problem may be avoided by synthesizing

* Corresponding author. Tel.: +86 010 62333765; fax: +86 010 62327878.
E-mail address: gewang@mater.ustb.edu.cn (G. Wang).

1381-1169/$ – see front matter © 2013 Elsevier B.V. All rights reserved.
http://dx.doi.org/10.1016/j.molcata.2013.04.019

superparamagnetic inorganic/functional polymer nanospheres via the miniemulsion polymerization. It is well known that polyvinyl pyridine can serve as a catalyst scaffold to immobilize transition metal complexes such as Re, Mo, Au, Cr by strong electrostatic interaction [11,12].

In the present work, superparamagnetic Fe_3O_4/P4VP composite nanospheres with multiple Fe_3O_4 cores embedded in a P4VP shell were synthesized successfully via miniemulsion polymerization. The composite nanospheres possess rich N-based functional groups without any surface modification and abundant Fe_3O_4 cores with a strong magnetic response to enhance separation efficiency. This structure is extremely beneficial to the immobilization and rapid recovery of homogeneous complex catalysts. The specific synthetic route is shown in Scheme 1. 4-Vinylpyridine monomer was polymerized on the surface of oleic acid (OA) modified Fe_3O_4 nanoparticles to form Fe_3O_4/P4VP composite nanospheres in which the Fe_3O_4 nanoparticles were homogenously dispersed into the P4VP backbone. The Fe_3O_4/P4VP composite nanospheres were used as support to immobilize $MoO_2(acac)_2$. To prepare olefin epoxide, a key chemical intermediate, with environment-friendly chemical methods, epoxidation of cis-cyclooctene with oxidant of aqueous H_2O_2 in the solvent of ethanol was chosen as a model system [4] to illustrate the use of our recoverable Fe_3O_4/P4VP-Mo catalyst. To the best of our knowledge, there has been no report about the preparation of composite nanospheres with multiple Fe_3O_4 cores embedded in a P4VP shell and its application as the catalyst support in a green epoxidation system.

2. Experimental

2.1. Materials

Oleic Acid (90%), 4-vinylpyridine (4-VP, 96%), divinyl-benzene (DVB, 80%), cis-cyclooctene (96%), styrene (96%), 2-methyl styrene (98%), nitrobenzene (98%), and $MoO_2(acac)_2$ (99%) were purchased from Alfa Aesar. Ferric chloride hexahydrate ($FeCl_3{\cdot}6H_2O$, AR), ferrous chloride tetrahydrate ($FeCl_2{\cdot}4H_2O$, AR), ammonium hydroxide aqueous solution (28%), *n*-hexane (AR), sodium dodecyl sulfate (SDS, AR), potassium persulfate (KPS, AR), ethanol (AR) and H_2O_2 (30%) were purchased from Beijing Chemical Reagents Company. 4-VP and DVB were distilled under reduced pressure before use. All other chemicals were used without further purification.

2.2. Characterization

Scanning electron microscope (SEM) images of samples were obtained with a ZEISS SUPRA55 instrument operated at an acceleration voltage of 10 kV. Transmission electron microscopy (TEM) images were obtained using a JEOL JEM-100CX II electron microscope operating at 200 kV. High-resolution transmission electromicroscopy (HRTEM) images were taken with a JEM-2010 at 200 kV. Fourier-transformed infrared spectra (FTIR) were recorded with a NICOLET 6700 infrared spectrophotometer using KBr pellet samples. The magnetization curves of samples were measured by a MPMS-XL superconducting quantum interference device (SQUID) at room temperature. The magnetite content of a dried sample was measured by a TGA instrument (Netzsch, model STA f409) with platinum pans, where about 40 mg of dried sample was placed in platinum pans and heated from room temperature to 900 °C at a heating rate of 10 °C/min under nitrogen atmosphere (flow rate 20 mL/min). X-ray photoelectron spectroscopy data was gained with PHI Quantera SXM. All spectra including C 1s, N 1s and Mo 3d were curve fitted and referenced to the C1s neutral peak at 284.8 eV. Powder X-ray diffraction (XRD) data were collected with a DSADVANCE diffractometer using Cu Ka radiation. Gas chromatography–mass spectrum was recorded using Agilent 7890A/5975C. HP-5MS column was used in GC, the injection temperature was 50 °C, and helium gas was used as carrier gas. Products were determined by GC–MS using internal standard technique, and nitrobenzene was used as an internal standard. Particle diameter and size distribution of samples were measured using a Malvern Zetasizer 3000HS at a fixed scattering angle of 90°. Mo content of supported catalysts was measured by inductively coupled plasma-atomic emission spectrometry (Varian VISTA-MPX).

2.3. Synthesis of OA modified Fe_3O_4 nanoparticles

Fe_3O_4 nanoparticles were synthesized according to an improved co-precipitation procedure [10]. $FeCl_3{\cdot}6H_2O$ (25.3 g) and $FeCl_2{\cdot}4H_2O$ (8.6 g) were dissolved in deionized (400 mL) water under nitrogen gas with vigorous stirring at 80 °C. First, 28 mL of ammonium hydroxide aqueous solution was rapidly added into the solution. Then OA (8 mL) were added dropwise into the above suspension within 16 min. The suspension was kept reacting at 80 °C for 1 h. After cooling to room temperature, the Fe_3O_4 nanoparticles were successively washed several times with deionized water and ethanol and then dried in a vacuum for 12 h at 40 °C.

2.4. Synthesis of Fe_3O_4/P4VP composite nanospheres

Fe_3O_4/P4VP nanospheres were synthesized via a miniemulsion polymerization method. In a typical procedure, *n*-hexane-based magnetite ferrofluid (4.8 g) with as-synthesized magnetite weight content of 40% was added into aqueous solution (110 g) containing SDS (0.14 g). The mixture was treated by 300 W ultrasound in an ice-water bath for 20 min to obtain miniemulsion and then transferred to a 250 mL four-neck flask with a stirrer, condenser and N_2 inlet. The miniemulsion was stirred for 30 min at 300 rpm in nitrogen atmosphere, followed by the addition of the mixture of 4-VP (1.32 mL) and DVB (a certain amount) under stirring for 120 min to allow the swelling of 4-VP and DVB into the miniemulsion. Then the reaction system was heated to 70 °C and 0.4 wt% KPS aqueous solution (10 mL) was added rapidly to initiate the polymerization. After polymerization had proceeded for 8 h, the formed Fe_3O_4/P4VP nanospheres were washed with ethanol six times and dried in a vacuum for 12 h at 40 °C.

2.5. Immobilization of $MoO_2(acac)_2$ on Fe_3O_4/P4VP nanospheres (Fe_3O_4/P4VP-Mo)

$MoO_2(acac)_2$ (1.0 g) was dissolved in ethanol (340 mL) under mechanical stirring. Fe_3O_4/P4VP composite nanoparticles (1.0 g) were then added into this solution and the system was refluxed at 70 °C for 72 h. The product (Fe_3O_4/P4VP-Mo) was magnetically separated, washed with ethanol several times and then dried in a vacuum for 12 h at 40 °C.

2.6. Catalytic epoxidation of cis-cyclooctene

In a typical procedure, the Fe_3O_4/P4VP-Mo catalyst (0.1 g), H_2O_2 (22 mmol), cis-cyclooctene (3.5 mmol), nitrobenzene (0.2 mmol) and ethanol (5 mL) were added into a 50 mL round bottom flask and put in a 60 °C Water Bath Shaker for 12 h under continuous shaking. After the reaction the catalyst was quickly recovered with a magnet, rinsed with ethanol, and dried in a vacuum for 12 h for the next cycle of catalysis under identical conditions. Products were quantified by gas chromatography-mass spectrum on Agilent 7890A/5975C, and nitrobenzene was used as an internal standard.

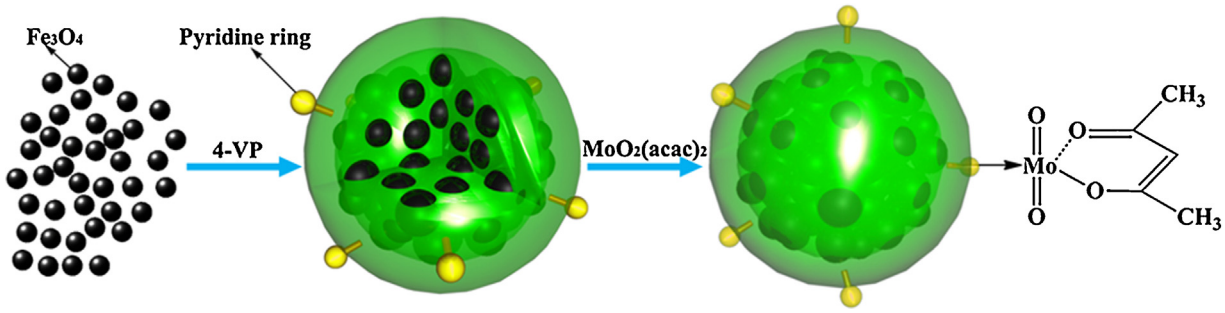

Scheme 1. Schematic illustration of the synthesis of composite Fe_3O_4/P4VP nanospheres and the immobilization of $MoO_2(acac)_2$.

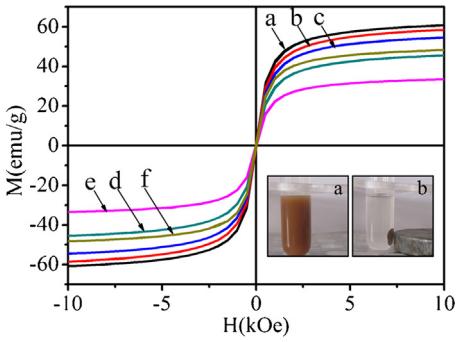

Fig. 1. Magnetization curves of samples at 300 K: the OA modified Fe_3O_4 (a), Fe_3O_4/P4VP nanospheres synthesized by various DVB concentrations from 0/8 (b), 1/8 (c), 2/8 (d), 4/8 (e) (molar ratio) based on 4-VP monomer, and Fe_3O_4/P4VP-Mo catalyst (f). Photos of the insets depict magnetic recycling of Fe_3O_4/P4VP-Mo catalyst (a: before applying the external magnetic field; b: ca. 5 s after applying the external magnetic field).

3. Results and discussion

3.1. Synthesis of Fe_3O_4/P4VP composite nanospheres

OA modified Fe_3O_4 nanoparticles were synthesized via an improved co-precipitation method reported previously [10]. The modification of Fe_3O_4 with OA may enhance the compatibility of the nanoparticles with organic monomer, which favours the encapsulation of polymer by miniemulsion polymerization [8,9]. XRD spectra (Fig. S1) indicate that the as-synthesized Fe_3O_4 nanoparticles have a cubic spinel structure. The average grain size calculated by Scherer's equation is about 11.5 nm, smaller than the critical size of Fe_3O_4 (ca. 30 nm) [13], which confirms the superparamagnetic nature of the as-synthesized Fe_3O_4 nanoparticles (Fig. 1a).

Fe_3O_4/P4VP composite nanospheres were prepared via miniemulsion polymerization. The nanospheres had unique core/shell architecture with multiple strong magnetic responsive cores and a functional polymeric shell. Abundant pyridine functional groups of P4VP may immobilize catalyst and promote catalytic activity as well due to their Lewis base characteristic for some specific reactions, such as epoxidation of olefins [4,11,14].

As shown in Fig. 2b, multiple black Fe_3O_4 nanoparticles were homogeneously embedded in the P4VP nanosphere, in which Fe_3O_4 nanoparticles corresponding to particles of ca.12 nm (Fig. 2a) were consistent with the result calculated according to Scherer's equation. The average size of the composite nanospheres with narrow size distribution was ca.180 nm (Fig. 2b). IR spectrum of the as-synthesized polymer composite nanospheres (Fig. S2b) also confirmed that OA-modified Fe_3O_4 nanoparticles were completely wrapped into cross-linked P4VP backbone. Absorption bands at 1597 cm^{-1}, 1540 cm^{-1}, 1414 cm^{-1}, 580 cm^{-1} were assigned to the C—N, C—C vibration modes of pyridine and benzene [15], and Fe—O of Fe_3O_4, corresponding to an absorption peak at 576 cm^{-1} [16] in FTIR spectra of OA-modified Fe_3O_4 nanoparticles (Fig. S2a), respectively.

The magnetization curves of synthesized samples are shown in Fig. 1. The magnetization curves of composite nanospheres exhibit no remanence at room temperature. Again, the results indicate their superparamagnetism, which is crucial for controllable flocculation and dispersion in solution in an external magnetic field [17]. The saturation magnetization value of composite nanosphere of 54.6 emu/g (Fig. 1c) ensures its rapid recoverability as catalyst support under an external magnetic field, and is much higher than that of other reported magnetic composite supports [5,18]. However, the value is slightly lower than that of OA-modified Fe_3O_4 nanoparticles (60.8 emu/g) (Fig. 1a) due to the capsulation of magnetic components into the P4VP.

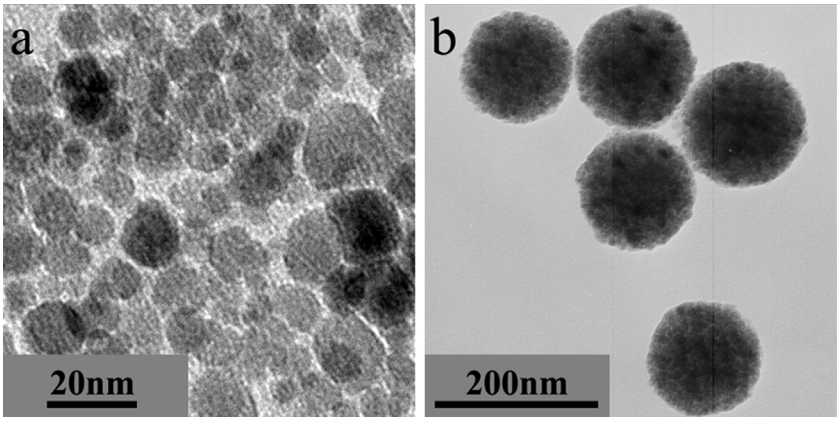

Fig. 2. HRTEM image of the OA modified Fe_3O_4 nanoparticles (a), TEM image of Fe_3O_4/P4VP nanospheres (b).

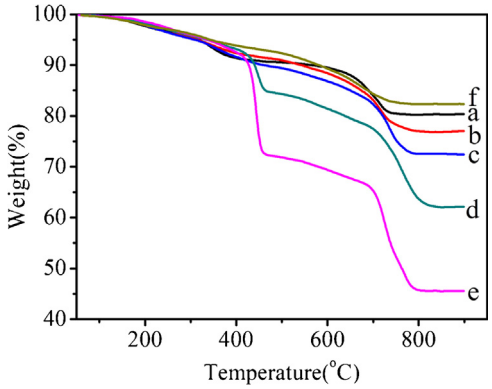

Fig. 3. TGA curves of the OA modified Fe_3O_4 nanoparticles (a), Fe_3O_4/P4VP nanospheres synthesized by various DVB concentrations from 0/8 (b), 1/8 (c), 2/8 (d), 4/8 (e) (molar ratio) based on 4-VP monomer, and Fe_3O_4/P4VP-Mo (f).

To optimize synthesis parameters, the effects of the ratio of DVB/4-VP, the concentration of magnetite ferrofluid, and the amount of the surfactant SDS on the structure of Fe_3O_4/P4VP composite nanospheres are discussed in detail as follows.

3.1.1. *Effect of the ratio of DVB/4-VP on the structure of Fe_3O_4/P4VP composite nanospheres*

It is well known that a cross-linking agent has a critical influence on the strength, elasticity and solvent resistance of polymer structure [19]. The effect of cross linker DVB amount on the structure, Fe_3O_4 content and magnetic response of as-synthesized magnetic polymer nanospheres was investigated in detail.

With the increase of DVB content, the Fe_3O_4 content and corresponding magnetic response of the composite nanospheres decreased significantly. Fig. 3b–e reveals the TGA results of Fe_3O_4/P4VP composite nanospheres synthesized by various DVB contents from 0/8 (b), 1/8 (c), 2/8 (d), 4/8 (e) (molar ratio) based on 4-VP monomer. Weight loss between 200 °C and 850 °C can be attributed to the decomposition of the OA and polymer structure. According to the residual weight of the TGA samples, the Fe_3O_4 content of as-synthesized composite nanospheres decreases from 77.13–72.44% to 62.31–45.66% as the DVB content gradually increases, consistent with the reduction trend in the saturation magnetization of those composite nanospheres. Similar to the magnetic hysteresis loop of OA-modified Fe_3O_4 nanoparticle, as-synthesized composite polymer nanospheres with various DVB concentrations keep their superparamagnetism (Fig. 1), which can be attributed to weak interaction between Fe_3O_4 nanoparticles evenly distributed into the polymer composite nanosphere framework. The saturation magnetization of the composite polymer nanospheres decreases from 58.5, 54.6, 45.6, to 33.4 emu/g (Fig. 1b–e) as DVB content is increased. This is due to the incorporation of more diamagnetic components into the composite nanospheres [8].

TEM images of Fe_3O_4/P4VP nanospheres (Fig. S3) indicate that OA-modified Fe_3O_4 nanoparticles are all well distributed in the P4VP framework. However, when the molar ratio of DVB/4-VP increases to 4/8 (Fig. S3d), significant aggregation is observed among as-synthesized composite nanospheres. High DVB content causes the degree of crosslinking of polymer chains to increase and endows the surface of the polymer nanospheres with excessive double bonds to enhance the probability of conglomeration and crosslinking between the composite polymer nanospheres [20].

Considering the further decrease in the magnetic response of composite nanospheres immobilizing catalysts and facile swollen nature of noncrosslinked polymer in organic solvent leading to leakage of magnetic cores from the polymer framework, as-synthesized polymer composite nanospheres with molar ratio of DVB/4-VP at 1/8 were chosen preliminarily as complex catalyst support.

3.1.2. *Effect of the concentration of magnetite ferrofluid on the structure of composite Fe_3O_4/P4VP nanospheres*

The concentration of magnetic fluid has an important impact on the magnetite content of as-synthesized Fe_3O_4/P4VP nanospheres for miniemulsion polymerization [9,21]. A higher concentration of magnetic fluid may produce Fe_3O_4/P4VP composite nanospheres with higher magnetite content, which will enhance the magnetic response of the composite nanospheres. As expected, according to the TGA results (Fig. S4), the magnetite content went up from 64.90%, 67.85%, to 72.44%, with an increase in concentration of magnetic fluid from 20%, 30%, to 40%. However, with a further increase in the concentration of magnetic fluid to 50%, there was no corresponding increase in the magnetite content of the as-synthesized composite nanospheres, which remained at 72.11% (Fig. S4d). With concentrations of magnetic fluid up to 50%, there were too many OA-modified Fe_3O_4 nanoparticles to disperse into *n*-hexane in preparation for magnetic fluid due to a minor discrepancy in the solubility parameter between OA(17.38(MPa)$^{1/2}$) [22] and *n*-hexane(14.9(MPa)$^{1/2}$) [22]. Because the magnetic response of as-synthesized composite nanospheres correlated positively with their magnetite content [8], composite nanospheres with stronger magnetic response are more suited to recovering the magnetic composite catalyst.

3.1.3. *Effect of the concentration of SDS on the structure of composite Fe_3O_4/P4VP nanospheres*

In order to optimize preparation parameters, the effects of SDS concentration on the structure of Fe_3O_4/P4VP composite nanospheres were further investigated. The SEM images (Fig. S5a–d) indicate the Fe_3O_4/P4VP nanospheres were all synthesized in various SDS concentrations, and DLS results show the mean particle diameter of as-synthesized Fe_3O_4/P4VP nanospheres decreased dramatically from 188.7 nm, 173.3 nm, 142.5 nm, to 124.9 nm as the SDS concentration was increased. However, the polydispersity index of the as-synthesized Fe_3O_4/P4VP nanospheres went up from 0.04, 0.03, 0.07, to 0.08 as the SDS content was increased, which means that the particle size distribution of the composite nanospheres became wider. The broad size distribution may lead to the loading of uneven amounts of catalyst on the composite nanospheres and an uneven magnetic response of the composite nanospheres. Considering that catalyst support demands a high specific surface area of composite nanospheres and consistent magnetic response demands a narrow size distribution, 2.92 wt% of SDS content based on magnetic fluid was chosen as the optimal synthesis parameter.

3.1.4. *Synthesis mechanism of Fe_3O_4/P4VP composite nanospheres via miniemulsion polymerization*

Monodispersed composite nanospheres with a strong magnetic response were obtained via miniemulsion polymerization. In the synthesis process, *n*-hexane-based magnetite ferrofluid dispersed into aqueous SDS solution was broken up into numerous nanoscale drops under strong ultrasonication. Magnetite content in the drops grew with the increase of magnetic fluid concentration, and the particle size of the resulting composite nanospheres decreased as SDS concentration increases. OA modified on the surface of Fe_3O_4 nanoparticle acted as an ultrahydrophobe to suppress Ostwald ripening to an extent, which makes nanoscale drops stable for a long time against their fusion.[9] The monomer 4-VP and crosslinker DVB were able to swell into those above droplets due to the similarity of their solubility parameters (22.5(MPa)$^{1/2}$ [23], 17.39(MPa)$^{1/2}$ [24], respectively) with that of *n*-hexane(14.9(MPa)$^{1/2}$). Then the

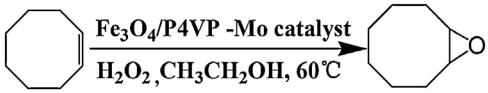

Scheme 2. Schematic illustration of catalytic epoxidation of cis-cyclooctene using Fe_3O_4/P4VP-Mo catalyst.

nanoscale miniemulsion droplets containing 4-VP and DVB as major nucleation sites were in situ polymerized to corresponding Fe_3O_4/P4VP composite nanospheres with the same size and narrow size distribution as the droplets. The increase in DVB content makes more nonmagnetic components swell into miniemulsion droplets, thus leading to the reduction of magnetite content in the resulting composite nanospheres.

Considering generally the effects of the DVB content, the SDS concentration and the concentration of magnetic fluid on the structure of the composite nanospheres, as-synthesized Fe_3O_4/P4VP composite nanospheres, with 1/8 molar ratio of DVB/4-VP, 2.92 wt% of the SDS concentration and 40% of the concentration of magnetic fluid, were chosen as catalyst support.

3.2. Immobilization of $MoO_2(acac)_2$ on Fe_3O_4/P4VP composite nanosphere

ICP-AES results also reveal that the Mo content of composite catalyst is 0.975 mmol/g, consistent with the TGA result (Fig. 3) that the residue weight of Fe_3O_4/P4VP-Mo (Fig. 3f, 82.55%) is higher than that of Fe_3O_4/P4VP (Fig. 3c, 72.44%), indicating the deposition of Mo species on Fe_3O_4/P4VP nanosphere support. Compared with the Fe_3O_4/P4VP nanospheres (Fig. S2b), the IR spectrum of Fe_3O_4/P4VP-Mo (Fig. S2c) exhibits the absorptions at 944, 905 cm^{-1} of vibration of Mo═O of $MoO_2(acac)_2$ [25], and the blue shift of C—N vibration absorption from 1598 to 1630 cm^{-1} [15], which confirms that $MoO_2(acac)_2$ was introduced to the Fe_3O_4/P4VP composite support.

The XPS spectra of samples (Fig. S6) also provide valuable information. Different from a single symmetrical N1s peak at binding energy 399.9 eV in Fe_3O_4/P4VP nanospheres (Fig. S6a), the N 1s spectrum of Fe_3O_4/P4VP-Mo catalyst (Fig. S6c) consists of three peaks at 398.4 eV, 399.6 eV, and 401.5 eV, corresponding to N atoms coordinated with Mo species [26], neutral N atoms of pyridine ring, and protonated N species [26], respectively. The Mo 3d spectrum of Fe_3O_4/P4VP-Mo catalyst (Fig. S6d) exhibits similar double peaks with that of $MoO_2(acac)_2$ (Fig. S6b). The above results confirm that Mo species was successfully immobilized on the Fe_3O_4/P4VP nanospheres, as shown in Scheme 1.

3.3. Catalytic epoxidation of cis-cyclooctene

As illustrated in Scheme 2, to evaluate the performance of Fe_3O_4/P4VP-Mo catalyst, green epoxidation of cis-cyclooctene, with aqueous H_2O_2 as green oxidant and ethanol as environmentally benign solvent, was chosen as a probe reaction. Organic oxidants such as *t*-butyl hydroperoxide [27] and noxious solvents such as acetonitrile [28] were often used for epoxidation of olefin, but the side effects of the reaction on the environment were much more difficult to eliminate. An alternative way of circumventing this drawback was to use aqueous H_2O_2 as green oxidant [29] and ethanol as an environmentally benign solvent. The hydrophilicity of P4VP in Fe_3O_4/P4VP nanospheres makes them easily disperse in green polar solvents (e.g. ethanol and water), which renders $MoO_2(acac)_2$ firmly anchored on the surface of the nanospheres catalyze substrates efficiently at a molecular level. At the same time, the strong magnetic response of Fe_3O_4/P4VP nanospheres ensures easy recoverability of heterogeneous catalyst. So far, some magnetic catalysts have been applied in the field of olefin epoxidation [5,18,30]. However, it is rare for magnetic catalyst to be used for the above field with both H_2O_2 and ethanol. Fe_3O_4/P4VP nanospheres as complex catalyst-scaffold provide a potentially extensive application for more liquid-phase chemical reactions using green solvents.

Table 1
The catalytic activity for epoxidation of cis-cyclooctene using H_2O_2 in ethanol catalyzed by Fe_3O_4/P4VP-Mo catalyst.[a,b]

Time (h)	3	6	9	12
Conv. (%)[c]	79.9	89.9	93.8	94.5
Sel. (%)[c]	99	99	99	99

[a] Reactions were conducted using cis-cyclooctene (3.50 mmol), 30 wt% H_2O_2 (22 mmol), catalyst (0.10 g, 0.098 mmol Mo), and ethanol (5.0 mL) at 60 °C.
[b] TOFs, described as mol epoxide/mol catalyst/time (h), can be calculated to 9.7 h^{-1} after 9 h reaction time and 39 h^{-1} after 10 min reaction time. Reactions were conducted using cis-cyclooctene (3.50 mmol), 30 wt% H_2O_2 (22 mmol), 1 mol% catalyst, and ethanol (5.0 mL) at 60 °C.
[c] The conversion and selectivity were determined by GC–MS with respect to an internal standard (nitrobenzene).

As shown in Table 1, Fe_3O_4/P4VP-Mo catalyst exhibits high conversion (94.5% at 12 h), lower than that of its corresponding homogenous counterpart (95% at 6 h), and excellent selectivity (99%) for this green epoxidation system. TOFs of the nanocatalyst has been also determined to 9.7 h^{-1}after 9 h reaction time and 39 h^{-1} after 10 min reaction time with 1 mol% catalyst, respectively. After the reaction is finished, Fe_3O_4/P4VP-Mo catalyst can be magnetically (ca. 5 s) recovered from the reaction system (inset in Fig. 1), which exhibits a strong response of this superparamagnetic catalyst. The specific saturation magnetization of this nanocomposite catalyst (48.3 emu/g, Fig. 1f) is far higher than that of magnetic composite catalyst reported in most previous literature [5,6,18,30,31].

Eight recycling tests of Fe_3O_4/P4VP-Mo catalyst for epoxidation of cis-cyclooctene were carried out. As shown in Table 2, 99% of selectivity of epoxidation retained and conversion of epoxidation decreased slightly over the eight consecutive runs, which confirms that Fe_3O_4/P4VP–Mo maintains its initial activity well. The content of Mo species in the recovered catalyst is 0.928 mmol/g, slightly lower than that in fresh catalyst (0.975 mmol/g), indicating that the loss of Mo active sites bound to P4VP is minimal. In view of similar morphologies (Fig. S5e–f) and IR spectra (Fig. S2c and d) for fresh and recovered catalyst, Fe_3O_4/P4VP composite nanospheres further turn out to be outstanding support for $MoO_2(acac)_2$.

Fe_3O_4/P4VP-Mo catalyst was further applied to the catalytic oxidation of aromatic olefins such as styrene and 2-methylstyrene under the same reaction conditions (Table 3). The main products were benzaldehyde and 2-methybenzaldehyde, respectively, with selectivity of more than 90%. The reason may be that styrene and

Table 2
Recycling tests of Fe_3O_4/P4VP-Mo catalyst in the epoxidation of cis-cyclooctene with H_2O_2 in ethanol.[a]

Cycle	Time (h)	Catalytic activity[b]	
		Conv. (%)[b]	Sel. (%)[b]
1st	12	94.5	99
2nd	12	92.1	99
3rd	12	91.6	99
4th	12	91.3	99
5th	12	90.7	99
6th	12	90.5	99
7th	12	90.5	99
8th	12	90.4	99

[a] Reactions were conducted using cis-cyclooctene (3.5 mmol), 30 wt% H_2O_2 (22 mmol), catalyst (0.1 g, 0.098 mmol Mo), and ethanol (5.0 mL) at 60 °C.
[b] The conversion and selectivity were determined by GC–MS with respect to an internal standard (nitrobenzene).

Table 3
Epoxidation of olefin with H_2O_2 in ethanol catalyzed by Fe_3O_4/P4VP-Mo catalyst.[a]

Entry	Time (h)	Alkene	Catalytic activity[b]	
			Conv. (%)	Sel. (%)
1	12	Cis-cyclootene	94.5	99
2	12	Styrene	83.3	92[c]
3	12	2-Methyl-styrene	91.7	95[d]

[a] Reactions were conducted using cis-cyclooctene (3.50 mmol), 30 wt% H_2O_2 (22 mmol), catalyst (0.10 g, 0.098 mmol), and ethanol (5.0 mL) at 60 °C.
[b] The conversion and selectivity were determined by GC–MS with respect to an internal standard (nitrobenzene).
[c] The main product is benzaldehyde.
[d] The main product is 2-methyl benzaldehyde.

2-methylstyrene were first oxidized by H_2O_2 to aromatic oxides and excessive H_2O_2 made aromatic oxides in the first step conversion to benzaldehyde and 2-methylbenzaldehyde [32]. The results show Fe_3O_4/P4VP-Mo catalyst is efficient for green preparation of benzaldehyde and 2-methybenzaldehyde with H_2O_2 as oxidant and ethanol as solvent.

4. Conclusions

In summary, we have synthesized novel superparamagnetic composite nanospheres with multiple Fe_3O_4 cores embedded in P4VP shell by miniemulsion polymerization. The magnetic response of composite nanospheres was tuned precisely by changing the DVB content or magnetic fluid concentration, and the size could be varied by SDS concentration. Both strong magnetic response and abundant pyridine rings enabled them to serve as easily recyclable support for the immobilization of catalysts. Fe_3O_4/P4VP composite nanospheres supported $MoO_2(acac)_2$ and exhibited good catalytic activity for green cis-cyclooctene epoxidation system and strong magnetic response (48.3 emu/g), and basically maintained initial catalytic activity after eight runs. While this paper focuses only on the immobilization of $MoO_2(acac)_2$ complex on Fe_3O_4/P4VP nanospheres, the basic design principles described here may not be limited to $MoO_2(acac)_2$ but should be expanded to other transition metal systems and noble metal nanoparticles; that is, carefully tuned superparamagnetic composite nanospheres could potentially play a crucial role as general easily recoverable support to anchor a wide variety of transition metal complex catalysts and noble metal nanoparticles.

Acknowledgements

We are grateful to the planned Science and Technology Project of Beijing, China (grant no. Z111103066611011), and the co-build project of Beijing Municipal Commission of Education for financial support.

Appendix A. Supplementary data

Supplementary data associated with this article can be found, in the online version, at http://dx.doi.org/10.1016/j.molcata.2013.04.019.

References

[1] (a) S. Kobayashi, M. Endo, S. Nagayama, J. Am. Chem. Soc. 121 (1999) 11229–11230;
(b) J.M. Thomas, W.J. Thomas, Principles and Practice of Heterogeneous Catalysis, VCH, Weinheim, 1997, pp. 1–10;
(c) X. Wang, K. Ding, J. Am. Chem. Soc. 126 (2004) 10524–10525;
(d) G. Grivani, S. Tangestaninejad, M.H. Habibi, V. Mirkhani, M. Moghadam, Appl. Catal. A Gen. 299 (2006) 131–136;
(e) J. Hagen, Industrial Catalysis: A Practical Approach, 2nd ed., Wiley-VCH, Weinheim, 2006, pp. 231–238.
[2] H.F. Rase, Handbook of Commercial Catalysts: Heterogeneous Catalysts, CRC, New York, 2000, pp. 13–35.
[3] (a) T. Maschmeyer, F. Rey, G. Sankar, J.M. Thomas, Nature 378 (1995) 159–162;
(b) J.M. Thomas, B.F.G. Johnson, R. Raja, G. Sankar, P.A. Midgley, Acc. Chem. Res. 36 (2003) 20–30;
(c) K. Feng, R.Y. Zhang, L.Z. Wu, B. Tu, M.L. Peng, L.P. Zhang, D.Y. Zhao, C.H. Tung, J. Am. Chem. Soc. 128 (2006) 14685–14690;
(d) C. Baleizão, H. Garcia, Chem. Rev. 106 (2006) 3987–4043;
(e) A. Thomas, M. Driess, Angew. Chem. Int. Ed. 48 (2009) 1890–1892;
(f) H.G. Ding, G. Wang, M. Yang, Y. Luan, Y.N. Wang, X.X. Yao, J. Mol. Catal. A Chem. 308 (2009) 25–31;
(g) V. Udayakumar, S. Alexander, V. Gayathri, Shivakumaraiah, K.R. Patil, B. Viswanathan, J. Mol. Catal. A Chem. 317 (2010) 111–117;
(h) B. Tamami, S. Ghasemi, Appl. Catal. A 393 (2011) 131–136;
(i) L.X. Li, Z.L. Liu, Q.L. Ling, D.X. Xing, J. Mol. Catal. A Chem. 353–354 (2012) 178–184.
[4] L.J. Cao, M. Yang, G. Wang, Y. Wei, D.B. Sun, J. Polym. Sci. Part A Polym. Chem. 48 (2010) 558–562.
[5] S. Shylesh, J. Schweizer, S. Demeshko, V. Schnemann, S. Ernst, W.R. Thiel, Adv. Synth. Catal. 351 (2009) 1789–1795.
[6] S. Shylesh, L. Wang, W.R. Thiel, Adv. Synth. Catal. 352 (2010) 425–432.
[7] (a) B. Fu, H.C. Yu, J.W. Huang, P. Zhao, J. Liu, L.N. Ji, J. Mol. Catal. A Chem. 298 (2009) 74–80;
(b) Y.H. Zhu, L.P. Stubbs, F. Ho, R.Z. Liu, C.P. Ship, J.A. Maguire, N.S. Hosmane, Chem. Catal. Chem. 2 (2010) 365–374;
(c) S. Wittmann, A. Schätz, R.N. Grass, W.J. Stark, O. Reiser, Angew. Chem. Int. Ed. 49 (2010) 1867–1870;
(d) A. Schätz, R.N. Grass, Q. Kainz, W.J. Stark, O. Reiser, Chem. Mater. 22 (2010) 305–310;
(e) S. Shylesh, W.R. Thiel, V. Schünemann, Angew. Chem. Int. Ed. 49 (2010) 3248–3459;
(f) V. Polshettiwar, R. Luque, A. Fihri, H.B. Zhu, M. Bouhrara, J.M. Basset, Chem. Rev. 111 (2011) 3036–3075.
[8] H. Xu, L.L. Cui, N.H. Tong, H.C. Gu, J. Am. Chem. Soc. 128 (2006) 15582–15583.
[9] T. Gong, D. Yang, J.H. Hua, W.L. Yang, C.C. Wang, J.Q. Lu, Colloids Surf. A 339 (2009) 232–239.
[10] X.Q. Liu, Y.P. Guan, Z.Y. Ma, H.Z. Liu, Langmuir 20 (2004) 10278–10282.
[11] P. Reyes, G. Borda, J. Gnecco, B.L. Rivas, J. Appl. Polym. Sci. 93 (2004) 1602–1608.
[12] (a) R. Saladino, V. Neri, A.R. Pelliccia, R. Caminiti, C. Sadun, J. Org. Chem. 67 (2002) 1323–1332;
(b) M.A. Rawashdeh-Omary, J.M. Loĭpez-de-Luzuriaga, M.D. Rashdan, O. Elbjeirami, M. Monge, M. Rodriĭguez-Castillo, A. Laguna, J. Am. Chem. Soc. 131 (2009) 3824–3825;
(c) G. Bayramoglu, M.Y. Arica, J. Hazard. Mater. 187 (2011) 221–231.
[13] J.P. Ge, Y.X. Hu, M. Biasini, W.P. Beyermann, Y.D. Yin, Angew. Chem. Int. Ed. 46 (2007) 4342–4345.
[14] J. Rudolph, L.K. Reddy, J.P. Chiang, K.B. Sharpless, J. Am. Chem. Soc. 119 (1997) 6189–6190.
[15] A.M. Lyons, M.J. Vasile, E.M. Pearce, J.V. Waszczak, Macromolecules 21 (1988) 3125–3134.
[16] S.J. Guo, S.J. Dong, E.K. Wang, Chem. Eur. J. 15 (2009) 2416–2424.
[17] C.W. Lim, I.S. Lee, Nano Today 5 (2010) 412–434.
[18] Y.H. Deng, Y. Cai, Z.K. Sun, J.C.L. Liu, J. Wei, W. Li, C. Liu, Y. Wang, D.Y. Zhao, J. Am. Chem. Soc. 132 (2010) 8466–8473.
[19] D.C. Sherrington, Chem. Commun. (1998) 2275–2286.
[20] M. Bacquet, C. Caze, J. Laureyns, C. Bremard, React. Polym. 9 (1988) 147–153.
[21] W.M. Zheng, F. Gao, H.C. Gu, J. Magn. Magn. Mater. 288 (2005) 403–410.
[22] C.M. Hansen, Hansen Solubility Parameters: A User's Handbook, 56, 2nd ed., CRC, New York, 2007, pp. 38.
[23] M.J. Yang, G.H. Hsiue, J. Appl. Polym. Sci. 39 (1990) 1475–1484.
[24] S. Yang, S.E. Shim, S. Choe, J. Polym. Sci. Part A Polym. Chem. 43 (2005) 1309–1311.
[25] S. Tangestaninejad, M. Moghadam, V. Mirkhani, I. Mohammadpoor-Baltork, K. Ghani, Inorg. Chem. Commun. 11 (2008) 270–274.
[26] L. Barrio, J.M. Campos-Martín, M. Pilar de Frutos, J.L.G. Fierro, Ind. Eng. Chem. Res. 47 (2008) 8016–8024.
[27] (a) H. Vrubela, K.J. Ciuffib, G.P. Riccib, F.S. Nunesa, S. Nakagaki, Appl. Catal. A 368 (2009) 139–145;
(b) A.C. Coelho1, S.S. Balula1, S.M. Bruno1, J.C. Alonso, N. Bion, P. Ferreira, M. Pillinger, A.A. Valente, J. Rocha, I.S. Gonçalves, Adv. Synth. Catal. 352 (2010) 1759–1769.
[28] (a) I. Garcia-Bosch, X. Ribas, M. Costas, Adv. Synth. Catal. 351 (2009) 348–352;
(b) K.F. Lin, O.I. Lebedev, G.V. Tendeloo, P.A. Jacobs, P.P. Pescarmona, Chem. Eur. J. 16 (2010) 13509–13518;
(c) K. Schröder, B. Join, A.J. Amali, K. Junge, X. Ribas, M. Costas, M. Beller, Angew. Chem. Int. Ed. 50 (2011) 1425–1429.
[29] K. Kamata1, K. Yonehara, Y. Sumida, K. Yamaguchi, S. Hikichi, N. Mizuno, Science 300 (2003) 964–966.
[30] M. Shokouhimehr, Y. Piao, J. Kim, Y. Jang, T. Hyeon, Angew. Chem. Int. Ed. 46 (2007) 7039–7043.
[31] (a) J.P. Ge, T. Huynh, Y.X. Hu, Y.D. Yin, Nano Lett. 8 (2008) 931–934;
(b) J.P. Ge, Q. Zhang, T.R. Zhang, Y.D. Yin, Angew. Chem. Int. Ed. 120 (2008) 9056–9060.
[32] X.G. Yang, S. Gao, Z.W. Xi, Org. Process Res. Dev. 9 (2005) 294–296.